Journal of Rehabilitation Sciences and Research

Journal Home Page: jrsr.sums.ac.ir

JRSR

Original Article

Optimal Strategy for Sit-to-Stand Movement Using Reinforcement Learning

Saeed Jamali[1], Sajjad Taghvaei[2], Seyyed Arash Haghpanah[2*]

[1]Department of Computer Engineering, Central Tehran Branch, Islamic Azad University, Tehran, Iran
[2]School of Mechanical Engineering, Shiraz University, Shiraz, Iran

ARTICLE INFO

ABSTRACT

Background: Sit-to-stand motion is a frequent and challenging task in daily life activities especially for elderly and disabled people. Central nervous system uses several strategies for sit-to-stand movement. Many studies have been conducted to understand the underlying basis of the optimal approach. Reinforcement learning (RL) is a suitable method for modeling the control strategies that occur in neuro-musculoskeletal system.

Methods: In this paper a dynamic model of human sit-to-stand was derived, and kinematic data of a healthy subject has been extracted in this task. An optimal control problem was formulated considering minimum energy and Q-Learning method has been utilized to find the optimal joint moments during sit to stand movement.

Results: The simulation results have been compared to the experimental data. The lower extremity joint angles have been simulated and tracked the actual human angles extracted from the experiments. Also the joints moments showed a satisfactory precision by the proposed approach.

Conclusion: An RL-based algorithm was used to model the human sit-to-stand, in which the model explores the state space with a Markov based approach and finds the best actions (joint moments) at each state (posture). In this approach the model successfully performs the task while consuming minimum energy. This was achieved by updating the algorithm in every trial using a Q-learning method.

2017© The Authors. Published by JRSR. All rights reserved.

Introduction

The population aging is an important issue even in developing countries. It has been reported that 10.5% of the Iranian people were over 60 years old in 2015. This population is going to increase to 21.7 % in 2050 [1]. This highly vulnerable group of society needs support for their daily life activities. Sit-to-stand movement is a frequent (four times per hour [2]) and important daily task. The performance of this movement declines with age which dramatically affects the independence of elderly people.

Consequently, various investigations have been conducted to explore the underlying mechanism of sit-to-stand movement [3, 4]. The previous studies can be classified into three main categories. The first category emphasizes on the musculoskeletal modeling of the sit-to-stand movement among healthy, elderly [5, 6] or disabled subjects [7]. In a systematic review, the main environmental factors that affect the performance of sit-to-stand are determined using the experimental background in this field [8]. In this category, the approach is mainly based on the experimental and statistical analysis of the acquired data. kinematics of sit-to-stand motion has been extracted using mode based inertial sensing based on a three segment model [9]. The results usually indicate the main factors that influence the performance of the

Corresponding author: Seyyed Arash Haghpanah, School of Mechanical Engineering, Shiraz University, Mula Sadra St., Shiraz, Iran.
Tel: +98 71 36133640; **Fax:** +98 71 36473533
E-mail: haghpanah@shirazu.ac.ir

movement such as sensation, speed, balance, and height of chair [10].

In the second group, the underlying muscle control strategy is investigated. The experimental data is utilized to extract the muscle synergies during the task [11]. Moreover the activation patterns of the muscles in sit-to-stand [12] are studied using the recorded electromyography (EMG) of the muscle modules involved in the motion [13].

In the third approach, a mathematical dynamic model is derived and the joint forces and moments are determined [14]. A control problem is usually defined and the control signals (usually the joint moments) are calculated such that the model output mimics the experimental data [15]. The muscular activation patterns are considered as the solution of an optimization problem [16].

In this paper, as a continuation of the previous works in the third category, the optimization problem is solved using reinforcement learning (RL) approach. RL techniques have been widely used in robotic applications especially when the problem is neither supervised nor unsupervised learning [17]. There has also been several studies on solving control problems with RL methodology [18, 19]. This strategy has been applied to find joint trajectories in a humanoid robot to go from crouch to stand position with minimizing power consumption [20]. Also in sequential human motions RL has been implemented to predict the movement [21]. Since the sit-to-stand task, more specifically, the muscle activation pattern, is learned by human, RL approach can be used to find the desired control pattern. The reward function can be defined such that the control system shows optimal performance.

In this paper a three-linkage dynamic model of human is proposed and the joint moments are determined using RL technique. The results are then compared with experimental data.

The organization of the paper is as follows: the dynamic model for STS motion is presented in section 2, the RL controller is proposed in section 3, the experimental results and discussions are presented in section 4, and section 5 contains the conclusion of the paper.

Methods

Dynamic Model

In order to model the human body during STS motion with fixed support, a linkage model with three segments representing shank, thigh and HAT (head and trunk) interconnected with revolute joints is used. The dynamic effects of the arms are neglected in this model. The segment lengths are denoted by l_i, i=1,2,3 in Figure 1, and the generalized coordinates are shown by φ_i, i=1,2,3 which are respectively the ankle, knee, and hip joint angles. The position of the ith link center of mass is identified by the distance d_i, i=1,2,3 measured from the distal joint as shown Figure 1.

The human dynamic model is obtained using Lagrange's equations:

$$\frac{d}{dt}\left(\frac{\partial L}{\partial \dot{q}_i}\right) - \frac{\partial L}{\partial q_i} = Q_i \tag{1}$$
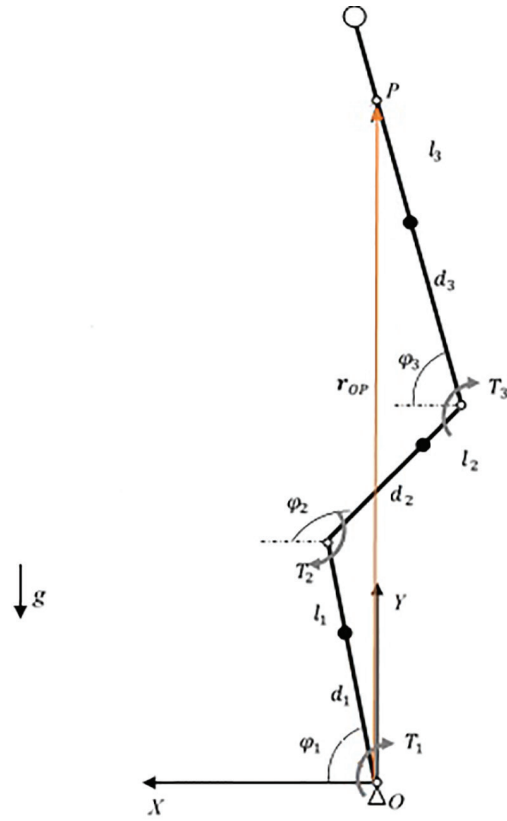

Figure 1: schematic diagram of the dynamic model.

wherein L is the Lagrangian, t is the time variable, q_i is the generalized coordinate, and Q_i is the generalized force/moment. Denoting by m_i the mass, J_i the moment of inertia, and v_i the velocity vector of the center of mass of the ith link, the kinetic energy, *KE*, and the potential energy, *PE*, of the model are, respectively, written as:

$$KE = \sum_{i=1}^{3}\left(\frac{1}{2}J_i\dot{\varphi}_i^2 + \frac{1}{2}m_i \boldsymbol{v}_i \cdot \boldsymbol{v}_i\right)$$

$$= \frac{1}{2}[J_1 + m_1 d_1^2 + (m_2+m_3)l_1^2]\dot{\varphi}_1^2 + \frac{1}{2}(J_2 + m_2 d_2^2 + m_3 l_2^2)\dot{\varphi}_2^2 + \frac{1}{2}(J_3 + m_3 d_3^2)\dot{\varphi}_3^2$$

$$+(m_3 l_1 l_2 + m_2 l_1 l_2)\dot{\varphi}_1\dot{\varphi}_2\cos(\varphi_2-\varphi_1) + m_3 l_2 d_3\dot{\varphi}_2\dot{\varphi}_3\cos(\varphi_3-\varphi_2) + m_3 l_1 d_3\dot{\varphi}_1\dot{\varphi}_3\cos(\varphi_3-\varphi_1) \tag{2}$$

$$PE = [m_1 d_1 + (m_2+m_3)l_1]g\sin\varphi_1 + (m_2 d_2 + m_3 l_2)g\sin\varphi_2 + m_3 g d_3\sin\varphi_3 \tag{3}$$

where g denotes the gravitational acceleration. The generalized force/moment is obtained through calculating the virtual work δW due to the set of virtual (rotational) displacements , $\delta\varphi_i$, i=1,2,3 as in the following:

$$\delta W = (T_1 - T_2)\delta\varphi_1 + (T_2 - T_3)\delta\varphi_2 + T_3\delta\varphi_3 \tag{4}$$

where T_i, i=1,2,3, is the applied torque at the *i*th joint. It is seen in Appendix A how Eqs. (1)- (4) lead to the following dynamic equations governing the sit-to-stand motion:

$$a_1\ddot{\varphi}_1 + a_4\ddot{\varphi}_2\cos(\varphi_2-\varphi_1) + a_6\ddot{\varphi}_3\cos(\varphi_3-\varphi_1) - a_4\dot{\varphi}_2^2\sin(\varphi_2-\varphi_1) - a_6\dot{\varphi}_3^2\sin(\varphi_3-\varphi_1)$$

$$+b_1\cos\varphi_1 = T_1 - T_2 \tag{5}$$

$$a_2\ddot{\varphi}_2 + a_4\ddot{\varphi}_1\cos(\varphi_2-\varphi_1) + a_5\ddot{\varphi}_3\cos(\varphi_3-\varphi_2) + a_4\dot{\varphi}_1^2\sin(\varphi_2-\varphi_1) - a_5\dot{\varphi}_3^2\sin(\varphi_3-\varphi_2)$$

$$+b_2\cos\varphi_2 = T_2 - T_3 \tag{6}$$

$$a_3\ddot{\varphi}_3 + a_6\ddot{\varphi}_1\cos(\varphi_3-\varphi_1) + a_5\ddot{\varphi}_2\cos(\varphi_3-\varphi_2) + a_6\dot{\varphi}_1^2\sin(\varphi_3-\varphi_1) + a_5\dot{\varphi}_2^2\sin(\varphi_3-\varphi_2)$$

$$+b_3\cos\varphi_3 = T_3 \tag{7}$$

where

$$a_1 = J_1 + m_1 d_1^2 + (m_2 + m_3) l_1^2$$

$$a_2 = J_2 + m_2 d_2^2 + m_3 l_2^2$$

$$a_3 = J_3 + m_3 d_3^2$$

$$a_4 = (m_2 + m_3) l_1 l_2$$

$$a_5 = m_3 l_2 d_3$$

$$a_6 = m_3 l_1 d_3 \tag{8}$$

$$b_1 = (m_1 d_1 + m_2 l_1 + m_3 l_1) g$$

$$b_2 = (m_2 d_2 + m_3 l_2) g$$

$$b_3 = m_3 d_3 g \tag{9}$$

The model parameters for different segments of the body such length, mass, center of mass, and moment of inertia are determined using the anthropometric data suggested by [22].

Reinforcement Controller

Reinforcement learning (RL) techniques are one of the most popular algorithms used to solve model-based or model-free control problems [18]. RL is a trial-and-error based method that does not require a database or detail prior knowledge of the model and desired trajectory unlike supervised learning methods [23]. There are several strategies to perform this trial-and-error exploration and exploitation among which Q-Learning is an optimal one [24].

The standard reinforcement learning model consists of an agent connected to its environment through action and perception. On each step of exploration the agent receives, from the environment, some indication of the current state as input; the agent then chooses an action to generate the output. The algorithm should generate actions that increase a reward function [17]. The agent is trained over time by systematic trial and error, using a wide variety of algorithms, namely Q-Learning method.

Q-Learning a model-free, online-based approach to implement roughly repeating politics. In Q-learning, a Q-table provides a kind of agent's knowledge after a Markov Decision Process (MDP) [25]. The action that the agent chooses depends on his action selection policy. By making any action immediately, the agent receives an reward from the environment, which should result in a Q-value update as Eq. 10 where $Q(s,a)$ is the Q-value of current state-action pair, $max_{a'} Q(s',a')$ is the action having maximum Q-value in state s', α is the learning rate, γ is the discount factor and r is the reward value received after taking action a in state s.

$$Q(s,a) \leftarrow Q(s,a) + \alpha[r + \gamma max_{a'} Q(s',a') - Q(s,a)] \tag{10}$$

A pseudo-code of Q-learning algorithm is shown in Table 1.

The generated Q-table from the above mentioned algorithm provides the optimal (best rewarded) action for any state of motion. The states of sit-to-stand motion are vectors in space $\mathbb{R}^3$ representing ϕ_1, ϕ_2, ϕ_3 discretized through the range of motion. The actions are vectors of the same size which indicate the increase, decrease or no change in the values of associated angles. The reward function (J) is based on the cost function of an optimal control problem as described by Eq. 11.

$$J = \frac{1}{2} \sum_{i=1}^{3} \left(\phi_i(t_f) - \phi_i^{des}(t_f) \right)^2 + \frac{1}{2} \int_0^{t_f} \sum_{i=1}^{3} r_i \tau_i^2 \, dt \tag{4}$$

In which the first term indicates the difference between the model posture and the human posture at standing position $^{(\phi_i^{des})}$ at final time (t_f), and the second term represents the consumed energy during the whole movement. The coefficients r_i are chosen such that there is a balance between the final posture difference and the consumed energy.

Table 1: Q-Learning Algorithm

1. Initiate arbitrarily all $Q(s,a)$ values;
2. Repeat (for each episode):
(a) Choose a random (initial) states;
(b) Repeat (for each step in the episode):
i.   Select an action $a \in A(s)$ according to the policy;
ii.   Execute the action a, receive immediate reward r, then observe the new state s';
iii. $Q(s,a) \leftarrow Q(s,a) + \alpha[r + \gamma max_{a'} Q(s',a') - Q(s,a)]$
iv. $s \leftarrow s'$
Until s is one of the goal states;
Until the desired number of episodes have been investigated.

Experiment

Experiments have been performed in order to extract the kinematics of the human sit-to-stand task and verify the proposed model with actual data. During each experiment, the angle of the ankle, knee and hip are derived using marker-based visual analysis (Figure 2). The STS motion is performed with the assistance of the fixed support which is the walker with activated brakes as shown in Figure 2. Four circular markers of different colors which were attached to the subjects' shoulder, ankle, knee and hip joints, were used to follow the kinematics of motion on the basis of the proposed three-linkage model. They were then asked to sit down on a chair and stand up with closed arms on the chest. The subjects were asked to repeat the motion for four successive times with proper rest time in between so that the data was not affected by the subjects' tiredness during the process.

In each experiment, the entire motion is recorded using an RGB camera. The visual data is recorded in 30 frames per second, and is then used to obtain the x,y positions of the joints in order to distinguish the circular markers.
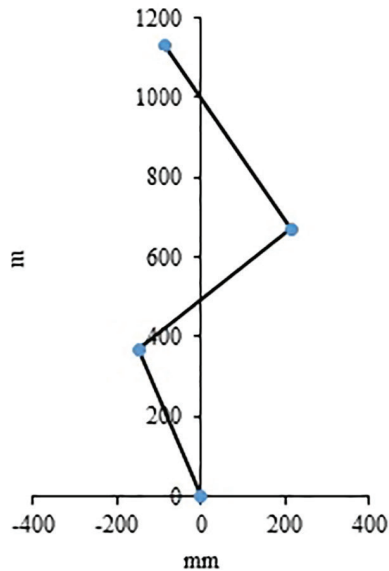
Figure 2: One of the case studies: (a) Schematic diagram of human body with specified joints and (b) Body movement during experiment.

Results

The proposed Q-Learning based controller is implemented on the three-linkage dynamic model and the results are compared with the experimental data acquired from human sit-to-stand motion. The proposed model successfully stands up from seated position and at the final states reach the desired human posture as shown in Figure 3.

Moreover, the generated joint torques are calculated and an average value of the applied joint moments are compared in Figure 4. The joint moments through the movement also indicate satisfactory performance of the model. This implies that the optimal Q-learning controller can be utilized to model such sit-to-stand movement.

Discussion

Using the Q-learning method, a dynamic model of sit-to-stand motion is controlled such that the task is successfully fulfilled with a similar pattern to human motion acquired from experimental data. This covers the kinematic aspect of resemblance in motion. The differences in joint angles in experiment and simulation are because of two reasons. Firstly, discretizing the state space is essential in QL-algorithm while the model is continuous. Secondly the muscles are not considered in the dynamic model which mainly affect the variations of ϕ_3. In the presented dynamic model, the trunk can remain vertical without applying any torque, while in the human body this requires activation of the trunk muscles.

From a kinetic point of view, the calculated average torque in the human motion equals to 35.5 *N.m* whereas the average torque of the Q-learning simulation is 35.8 *N.m*. This shows satisfactory compatibility between the proposed model and the experimental data according to dynamic behavior.

In a similar work by Edibol et. al. the Q-learning method was applied to control a humanoid robot in sit-to-stand motion [9]. Their goal was to reduce the power consumption during the task. For a 4.3kg NAO robot, they reported a reduction of average torque from 0.53 *N.m* to 0.49 *N.m* using Q-learning algorithm. In comparison to our study, their work is focusing on power reduction while we try to mimic the experimental results
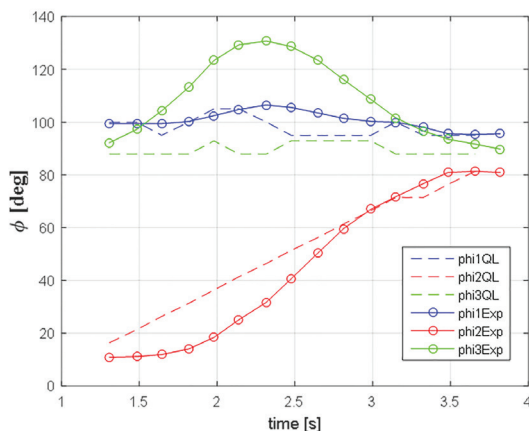

Figure 3: Variations of angles of the proposed model (phiQL) and the ones recorded in experiments (phiExp)
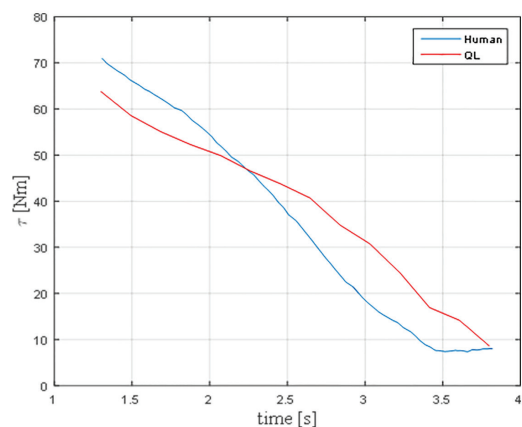

Figure 4: The average joint torques during the experiments with respect to time as calculated from the model (QL) and experiments (Human)

considering the optimal behavior of human motion. These are both achieved by adjusting the reward function in the reinforcement algorithm. Therefore the Q-learning approach can be utilized for various goals by defining different reward functions for the same task.

As a limitation of this study, the learning approach is based on a discrete state space while the actual task in happening in a continuous manner. This can be improved by implementing new continuous based learning approaches such as deep reinforcement learning [26].

In this study a linkage model was implemented for describing the motion, musculoskeletal models can be used to declare the sit-to-stand mechanism more precisely for future works. The contribution of each muscle in joint moments can be determined using the learning methods and compared to the EMG of the muscles obtained from the experiments.

Conclusion

A three linkage dynamic model of sit-to-stand movement was proposed. The joint moments applied at ankle, knee and hip were considered as the control inputs that can fulfill the movement. These values were determined such that the model successfully performs the task while consuming minimum energy. This was achieved through an RL-based algorithm in which the model explores the state space with a Markov based approach and finds the best actions (joint moments) at each state (posture). The algorithm is updated in every trial by a Q-learning method. The results were compared with experimental data captured by RGB camera. The simulation results show satisfactory performance of the proposed controller.

Conflict of interest: None declared.

References

1. Noroozian M. The elderly population in iran: an ever growing concern in the health system. Iranian journal of psychiatry and behavioral sciences. 2012;6(2):1.
2. Yamasaki HR, Kambara H, Koike Y. Dynamic optimization of the sit-to-stand movement. Journal of applied biomechanics. 2011;27(4):306-13.
3. Błażkiewicz M, Wiszomirska I, Wit A. A new method of determination of phases and symmetry in stand-to-sit-to-stand movement. International journal of occupational medicine and environmental health. 2014;27(4):660-71.
4. An Q, Ishikawa Y, Nakagawa J, Oka H, Yamakawa H, Yamashita A, et al., editors. Analysis of contribution of muscle synergies on sit-to-stand motion using musculoskeletal model. Advanced Robotics and its Social Impacts (ARSO), 2013 IEEE Workshop on; 2013: IEEE.
5. Schlicht J, Camaione DN, Owen SV. Effect of intense strength training on standing balance, walking speed, and sit-to-stand performance in older adults. The Journals of Gerontology Series A: Biological Sciences and Medical Sciences. 2001;56(5):M281-M6.
6. Faria CDCdM, Saliba VA, Teixeira-Salmela LF. Musculoskeletal biomechanics in sit-to-stand and stand-to-sit activities with stroke subjects: a systematic review. Fisioterapia em movimento. 2010;23(1):35-52.
7. Cachia C. A Biomechanical Analysis of the Sit-to-stand Transfer in Parkinson's Disease: ProQuest; 2008.
8. Janssen WG, Bussmann HB, Stam HJ. Determinants of the sit-to-stand movement: a review. Physical therapy. 2002;82(9):866-79.
9. Elibol E, Calderon J, Llofriu M, Quintero C, Moreno W, Weitzenfeld A, editors. Power usage reduction of humanoid standing process using q-learning. Robot Soccer World Cup; 2015: Springer.
10. Lord SR, Murray SM, Chapman K, Munro B, Tiedemann A. Sit-to-stand performance depends on sensation, speed, balance, and psychological status in addition to strength in older people. The Journals of Gerontology Series A: Biological Sciences and Medical Sciences. 2002;57(8):M539-M43.
11. An Q, Ishikawa Y, Funato T, Aoi S, Oka H, Yamakawa H, et al. Muscle synergy analysis of human standing-up motion using forward dynamic simulation with four body segment model. Distributed Autonomous Robotic Systems: Springer; 2016. p. 459-71.
12. Cheng P-T, Chen C-L, Wang C-M, Hong W-H. Leg muscle activation patterns of sit-to-stand movement in stroke patients. American journal of physical medicine & rehabilitation. 2004;83(1):10-6.
13. Goulart FR-d-P, Valls-Solé J. Patterned electromyographic activity in the sit-to-stand movement. Clinical neurophysiology. 1999;110(9):1634-40.
14. Roberts PD, McCollum G. Dynamics of the sit-to-stand movement. Biological cybernetics. 1996;74(2):147-57.
15. Taghvaei S, Tavasoli A, Feizi N, Rajestari Z, Abdi M. A control-oriented dynamic model for sit-to-stand motion with fixed support. Proceedings of the Institution of Mechanical Engineers, Part K: Journal of Multi-body Dynamics. 2017:1464419317731059.
16. Kuželički J, Žefran M, Burger H, Bajd T. Synthesis of standing-up trajectories using dynamic optimization. Gait & posture. 2005;21(1):1-11.
17. Kaelbling LP, Littman ML, Moore AW. Reinforcement learning: A survey. Journal of artificial intelligence research. 1996;4:237-85.
18. Barto AG. Reinforcement learning control. Current opinion in neurobiology. 1994;4(6):888-93.
19. Bagnell JA, Schneider JG, editors. Autonomous helicopter control using reinforcement learning policy search methods. Robotics and Automation, 2001 Proceedings 2001 ICRA IEEE International Conference on; 2001: IEEE.
20. Musić J, Kamnik R, Munih M. Model based inertial sensing of human body motion kinematics in sit-to-stand movement. Simulation Modelling Practice and Theory. 2008;16(8):933-44.
21. Kleijn R, Kachergis G, Hommel B. Predictive Movements and Human Reinforcement Learning of Sequential Action. Cognitive science. 2018.
22. Hall SJ, Sciences H. Basic biomechanics. 7 ed. United States: McGraw Hill Higher Education; 2014 2014/03/01.
23. Sutton RS, Barto AG. Reinforcement learning: An introduction: MIT press Cambridge; 1998.
24. Watkins CJ, Dayan P. Q-learning. Machine learning. 1992;8(3-4):279-92.
25. Bellman R. A Markovian decision process. Journal of Mathematics and Mechanics. 1957:679-84.
26. Lillicrap TP, Hunt JJ, Pritzel A, Heess N, Erez T, Tassa Y, et al. Continuous control with deep reinforcement learning. arXiv preprint arXiv:150902971. 2015.

Appendix A: Intermediate steps in deriving Equations (6)-(8)
Using Equations (2) and (3), the Lagrangian is written as

$$L = KE - PE$$

(A.1)

$$= \frac{1}{2} a_1 \dot{\varphi}_1^2 + \frac{1}{2} a_2 \dot{\varphi}_2^2 + \frac{1}{2} a_3 \dot{\varphi}_3^2 + a_4 \dot{\varphi}_1 \dot{\varphi}_2 \cos(\varphi_2 - \varphi_1) + a_5 \dot{\varphi}_2 \dot{\varphi}_3 \cos(\varphi_3 - \varphi_2)$$

$$+ a_6 \dot{\varphi}_1 \dot{\varphi}_3 \cos(\varphi_3 - \varphi_1) + b_1 \sin \varphi_1 + b_2 \sin \varphi_2 + b_3 \sin \varphi_3$$

The following differentiation results are then obtained based on Equation (A.1)

$$
\begin{cases}
\frac{\partial L}{\partial \dot{\varphi}_1} = a_1 \dot{\varphi}_1 + a_4 \dot{\varphi}_2 \cos(\varphi_2 - \varphi_1) + a_6 \dot{\varphi}_3 \cos(\varphi_3 - \varphi_1) \\
\frac{d}{dt}\left(\frac{\partial L}{\partial \dot{\varphi}_1}\right) = a_1 \ddot{\varphi}_1 + a_4 \ddot{\varphi}_2 \cos(\varphi_2 - \varphi_1) + a_6 \ddot{\varphi}_3 \cos(\varphi_3 - \varphi_1) - a_4 \dot{\varphi}_2(\dot{\varphi}_2 - \dot{\varphi}_1)\sin(\varphi_2 - \varphi_1) \\
\qquad\qquad - a_6 \dot{\varphi}_3(\dot{\varphi}_3 - \dot{\varphi}_1)\sin(\varphi_3 - \varphi_1) \\
\frac{\partial L}{\partial \varphi_1} = a_4 \dot{\varphi}_1 \dot{\varphi}_2 \sin(\varphi_2 - \varphi_1) + a_6 \dot{\varphi}_1 \dot{\varphi}_3 \sin(\varphi_3 - \varphi_1) - b_1 \cos \varphi_1 \\
\frac{\partial L}{\partial \dot{\varphi}_2} = a_2 \dot{\varphi}_2 + a_4 \dot{\varphi}_1 \cos(\varphi_2 - \varphi_1) + a_5 \dot{\varphi}_3 \cos(\varphi_3 - \varphi_2) \\
\frac{d}{dt}\left(\frac{\partial L}{\partial \dot{\varphi}_2}\right) = a_2 \ddot{\varphi}_2 + a_4 \ddot{\varphi}_1 \cos(\varphi_2 - \varphi_1) + a_5 \ddot{\varphi}_3 \cos(\varphi_3 - \varphi_2) - a_4 \dot{\varphi}_1(\dot{\varphi}_2 - \dot{\varphi}_1)\sin(\varphi_2 - \varphi_1) \\
\qquad\qquad - a_5 \dot{\varphi}_3(\dot{\varphi}_3 - \dot{\varphi}_2)\sin(\varphi_3 - \varphi_2) \\
\frac{\partial L}{\partial \varphi_2} = -a_4 \dot{\varphi}_1 \dot{\varphi}_2 \sin(\varphi_2 - \varphi_1) + a_5 \dot{\varphi}_2 \dot{\varphi}_3 \sin(\varphi_3 - \varphi_2) - b_2 \cos \varphi_2 \\
\frac{\partial L}{\partial \dot{\varphi}_3} = a_3 \dot{\varphi}_3 + a_5 \dot{\varphi}_2 \cos(\varphi_3 - \varphi_2) + a_6 \dot{\varphi}_1 \cos(\varphi_3 - \varphi_1) \\
\frac{d}{dt}\left(\frac{\partial L}{\partial \dot{\varphi}_3}\right) = a_3 \ddot{\varphi}_3 + a_5 \ddot{\varphi}_2 \cos(\varphi_3 - \varphi_2) + a_6 \ddot{\varphi}_1 \cos(\varphi_3 - \varphi_1) - a_5 \dot{\varphi}_2(\dot{\varphi}_3 - \dot{\varphi}_2)\sin(\varphi_3 - \varphi_2) \\
\qquad\qquad - a_6 \dot{\varphi}_1(\dot{\varphi}_3 - \dot{\varphi}_1)\sin(\varphi_3 - \varphi_1) \\
\frac{\partial L}{\partial \varphi_3} = -a_5 \dot{\varphi}_2 \dot{\varphi}_3 \sin(\varphi_3 - \varphi_2) - a_6 \dot{\varphi}_1 \dot{\varphi}_3 \sin(\varphi_3 - \varphi_1) - b_3 \cos \varphi_3
\end{cases}
$$

(A.2)

In addition, the generalized forces are obtained, using Equation (4), as follows

$$
\begin{cases}
Q_1 = \frac{\partial(\delta W)}{\partial(\delta \varphi_1)} = T_1 - T_2 + f \frac{\partial r}{\partial \varphi_1} \\
Q_2 = \frac{\partial(\delta W)}{\partial(\delta \varphi_2)} = T_2 - T_3 + f \frac{\partial r}{\partial \varphi_2} \\
Q_3 = \frac{\partial(\delta W)}{\partial(\delta \varphi_3)} = T_3 + f \frac{\partial r}{\partial \varphi_3}
\end{cases}
$$

(A.3)

where

$$\frac{\partial r}{\partial \varphi_i} = \frac{-l_i \sin \varphi_i \left(\sum_{j=1}^{3} l_j \cos \varphi_j - X_Q\right) + l_i \cos \varphi_i \left(\sum_{j=1}^{3} l_j \sin \varphi_j - Y_Q\right)}{\sqrt{\left(\sum_{j=1}^{3} l_j \cos \varphi_j - X_Q\right)^2 + \left(\sum_{j=1}^{3} l_j \sin \varphi_j - Y_Q\right)^2}}$$

(A.4)

for *i*=1,2,3. The dynamic Equations (6)-(8) are then achieved by setting $q_i = \varphi_i$, *i*=1,2,3, and substituiting Equations (A.2) and (A.3) into Equation (1).